

Lawrence Berkeley National Laboratory

LBL Publications

Title

A periodic metallo-supramolecular polymer from a flexible building block: self-assembly and photocatalysis for organic dye degradation

Permalink

<https://escholarship.org/uc/item/7m56n462>

Journal

Science China Chemistry, 62(12)

ISSN

1674-7291

Authors

Li, Xiong-Fei
Liu, Xu-Bo
Chao, Jin-Yu
[et al.](#)

Publication Date

2019-12-01

DOI

10.1007/s11426-019-9600-2

Peer reviewed

A periodic metallo-supramolecular polymer from a flexible building block: self-assembly and photocatalysis for organic dye degradation

Xiong-Fei Li,¹ Xu-Bo Liu,¹ Jin-Yu Chao,¹ Ze-Kun Wang,¹ Faiz-Ur Rahman,^{1*} Hui Wang,¹ Dan-Wei Zhang¹ & Yi Liu^{2*} and Zhan-Ting Li^{1*}

¹Department of Chemistry, Shanghai Key Laboratory of Molecular Catalysis and Innovative Materials, Fudan University, 2205 Songhu Road, Shanghai 200438, China

²The Molecular Foundry, Lawrence Berkeley National Laboratory, One Cyclotron Road, Berkeley, California 94720, USA

Received ***; accepted ***; published online ***

A water-soluble metallo-supramolecular polymer **MSP-f-6Np**, which possesses a regular pore aperture of 1.4 nm, has been assembled from a structurally flexible naphthalene-appended [Ru(bipy)₃]²⁺ complex and cucurbit[8]uril. As the first periodic metallo-supramolecular polymer formed by a flexible building block, **MSP-f-6Np** exhibits a hydrodynamic diameter of 122 and 164 nm at 0.1 and 2.0 mM of the monomer concentrations. Synchrotron small angle X-ray scattering experiments confirm that **MSP-f-6Np** possesses porosity periodicity in both the solution and solid states. Compared with a control, the new highly ordered porous system displays enhanced photocatalytic activity for the degradation of organic dyes.

supramolecular polymer, structural flexibility, porosity periodicity, cucurbit[8]uril, photocatalysis, organic dye degradation

Citation: Li XF, Chao JY, Wang ZK, Rahman FU, Wang H, Zhang DW, Liu Y, Li ZT A periodic metallo-supramolecular polymer with flexible Ru²⁺-cored monomers: self-assembly and photocatalysis for organic dye degradations. *Sci China Chem*, ***, doi: ***

1 Introduction

Since the first report of supramolecular polymers that were generated from linear monomers driven by multiple hydrogen bonds [1], this family of soft matters has received increasing attention due to their unique features such as reversible formation and modulated structures and properties [2–15]. It has been established that multi-armed monomers can allow for the formation of three-dimensional (3D) supramolecular networks that exhibit increased stability through multivalence [16–19]. However, efficient control of molecular monomers into well-defined pores in solution has

been a challenge [20,21], even though in the past two decades periodic porous solid materials, such as metal-organic frameworks [22–26] and covalent-organic frameworks [27–30], have been extensively exploited for a variety of properties and functions.

We have recently reported that [Ru(bpy)₃]²⁺-derived (bpy: 2,2'-bipyridine) rigid precursors co-assemble with cucurbit[8]uril (CB[8]) to form periodic metal-cored supramolecular organic frameworks in water [31,32], which is driven by the encapsulation of CB[8] for the dimers of the aromatic arms that are attached to the [Ru(bipy)₃]²⁺ cores [33–36]. As a special kind of regular metallo-supramolecular

*Corresponding authors (emails: faizurrahman@fudan.edu.cn, yliu@lbl.gov, and ztli@fudan.edu.cn.)
© Science China Press and Springer-Verlag Berlin Heidelberg 2015

polymers (MSPs) [37–41], these self-assembled frameworks have been revealed as porous homogeneous catalysts for visible light-initiated proton reduction to hydrogen. Given the fact that most of reported supramolecular polymers consisting of flexible building blocks can only form amorphous structures, we were interested in developing efficient strategies for realizing the regularity of this kind of self-assembled architectures, because ordered arrangement of polymer backbones has been an important approach for enhancing specific properties or functions of polymers [42–44]. Herein we describe that a structurally flexible complex that contains a $[\text{Ru}(\text{bpy})_3]^{2+}$ core and six appended naphthalene (Np) arms can co-assemble with CB[8] in water to form a three-dimensional metallo-supramolecular polymer that possesses porosity regularity in both the solution and solid state. We further show that this porosity regularity can remarkably enhance the homo- and heterogeneous photocatalytic activity of the incorporated $[\text{Ru}(\text{bpy})_3]^{2+}$ complexes for the degradation of organic dyes.

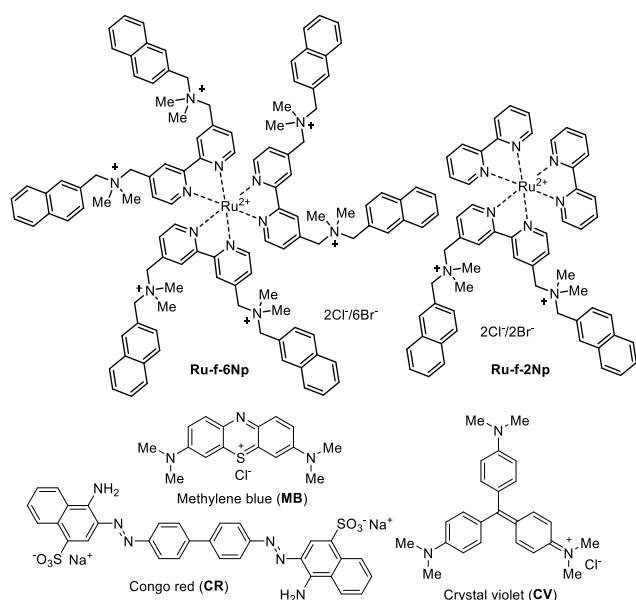
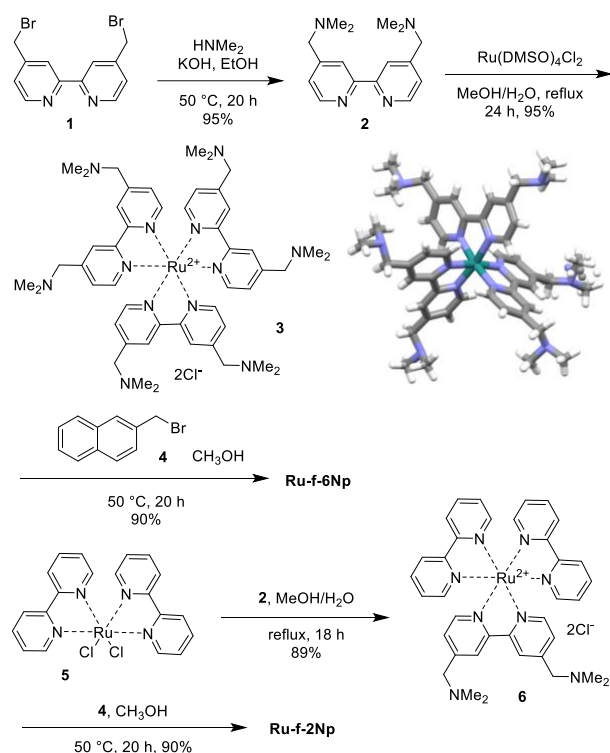


Figure 1 The structures of compounds **Ru-f-6Np**, **Ru-f-2Np**, methylene blue, congo red, and crystal violet.

2 Results and discussion

The encapsulation of CB[8] for aromatic dimers is a robust binding pattern for the formation of advanced supramolecular entities in water [33–36]. Several groups have utilized CB[8] encapsulation-enhanced Np dimerization to generate discrete supramolecular polymers [45]. To reach higher structural ordering for MSPs, we designed and prepared six-armed Ru^{2+} -based monomer **Ru-f-6Np** and control **Ru-f-2Np** (Figure 1), whose $[\text{Ru}(\text{bipy})_3]^{2+}$ cores were attached with six or two Np units through the flexible $-\text{CH}_2\text{NMe}_2+\text{CH}_2-$ linkers, respectively. Their synthetic routes are provided in Scheme 1. For the synthesis of **Ru-f-**

6Np, compound **1** was first reacted with dimethylamine to afford **2** in 95% yield. The pyridine derivative was then treated with $\text{Ru}(\text{DMSO})_2\text{Cl}_2$ to produce **3** in 95% yield. Finally, compound **3** was reacted with **4** to produce **Ru-f-6Np** in 90% yield. For the preparation of **Ru-f-2Np**, compound **6** was first prepared in 89% yield from the reaction of **2** and **5** and then reacted with **4** to afford **Ru-f-2Np** in 90% yield. Both **Ru-f-6Np** and **Ru-f-2Np** were highly soluble in water (>8.0 mM). The crystal structure of **3** revealed a symmetric octahedral feature for the complex core (Scheme 1), which is the key factor for the regularity of supramolecular metal-organic frameworks formed from rigid Ru^{2+} -complex prototypes [31,32].



Scheme 1 The synthesis of compounds **Ru-f-6Np** and **Ru-f-2Np** and the crystal structure (CCDC no.) of intermediate **3**.

CB[8] has a very limited solubility in water (<0.01 mM) [46]. Stirring its suspension (3 equiv relative to **Ru-f-6Np**) in the solution of **Ru-f-6Np** (3.0 mL) in water at room temperature for 14 days led to complete dissolution of CB[8]. This process could be finished in 2 hours at 100 °C. The resolution of the ^1H NMR spectrum of **Ru-f-6Np** in D_2O was notably lower than that of **Ru-f-2Np** (Figures S1 and S2, ESI), which reflects increased intermolecular stacking of the hydrophobic Np moieties as a result of the larger multivalence of the six Np units [16–19]. Upon binding CB[8], the resolution of both samples decreased remarkably (Figures S1 and S2, ESI). Job's plot obtained by fluorescence quenching experiments supported a 1:3 and 1:1 binding

stoichiometry for the two Ru_2^+ complexes and CB[8] (Figure S3, ESI), respectively, which were consistent with the established 2:1 binding motif between the Np units and CB[8] [40–42].

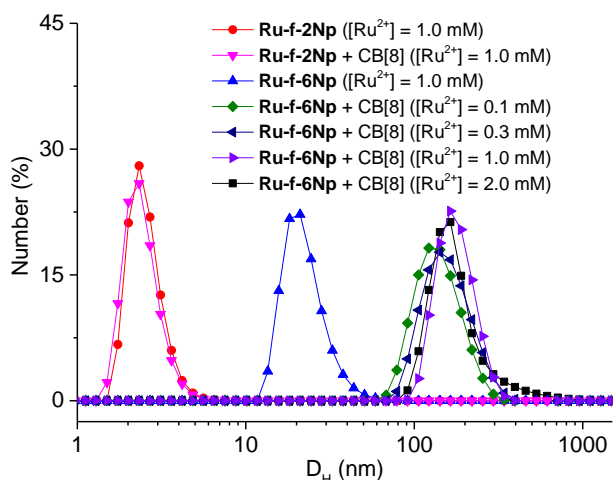


Figure 2 DLS profile of compounds **Ru-f-6Np** and **Ru-f-2Np** and their mixture with CB[8] (1:3 and 1:1) at different concentrations in water at 25 °C.

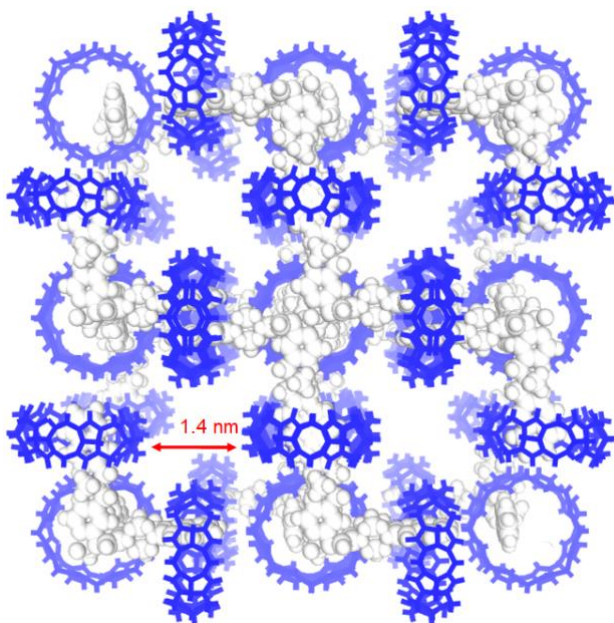


Figure 3 Model of periodic 3D metal-supramolecular polymer **MSP-f-6Np** formed by **Ru-f-6Np** and CB[8] (1:3), which has a pore aperture of 1.4 nm. The structure was obtained by Materials Studio 7.0.

2D diffusion ordered spectroscopic (DOSY) ^1H NMR experiment for the solution of **Ru-f-6Np** and CB[8] (1:3) in D_2O afforded a diffusion coefficient (D) of $3.2 \times 10^{-11} \text{ m}^2 \text{ s}^{-1}$ (Figure S4, ESI), which is comparable to that of the mixture obtained from a rigid prototypic precursor [28], supporting that the two components formed larger supramolecular entities. Dynamic light scattering (DLS) experiments for **Ru-**

f-2Np and **Ru-f-6Np** and their 1:1 or 1:3 mixture with CB[8] in water at $[\text{Ru}_2^+] = 1.0 \text{ mM}$ gave rise to a hydrodynamic diameter (D_H) of 2.3, 20, 2.5 and 151 nm, respectively (Figure 2). It can be found that the values of **Ru-f-2Np** and its 1:1 mixture with CB[8] were small, reflecting that the two molecules did not form large supramolecular aggregates. The relatively large value of pure **Ru-f-6Np** indicated that strong aggregation occurred due to intermolecular stacking of the appended hydrophobic Np units. Remarkably, the 1:3 mixture of **Ru-f-6Np** and CB[8] afforded a pronouncedly larger value of 151 nm. At $[\text{Ru}_2^+] = 0.1 \text{ mM}$ and 2.0 mM , the D_H values were 122 and 164 nm, respectively. The value at $[\text{Ru}_2^+] = 2.0 \text{ mM}$ was comparable to that of the rigid prototypic **Ru-r-6PhPy** at the identical Ru_2^+ concentration [28]. All these results supported that new large supramolecular entities (**MSP-f-6Np**, Figure 3) were generated within the studied concentration range.

Isothermal titration calorimetric (ITC) experiments were conducted by gradually adding the complexes to the aqueous solution of CB[8]. Apparent association constants K_{a1} and K_{a2} for the complexation of CB[8] for the first and the second Np unit were thus derived. For **Ru-f-2Np**, the values were $1.58 (\pm 0.41) \times 10^6$ and $1.83 (\pm 0.32) \times 10^4 \text{ M}^{-1}$, whereas for **Ru-f-6Np**, the values were $7.23 (\pm 0.46) \times 10^6$ and $7.91 (\pm 0.31) \times 10^4 \text{ M}^{-1}$ (Figure S5, ESI). The enthalpy changes (ΔH) related to the two 1:2 complexes were thus calculated to be $-16.5 (\pm 2.67)$ and $-53.4 (\pm 5.58) \text{ kcal}$, respectively, whereas the entropy changes ($-\text{T}\Delta S$) were determined to be -6.02 and -37.3 kcal , respectively. The larger values of **Ru-f-6Np** reasonably reflected the multivalence of the binding of its six Np units with CB[8], which led to the formation of the large supramolecular entities. In both cases, the enthalpic contribution was smaller than the entropic contribution, which was consistent with the high-energy water model proposed for the encapsulation of cucurbiturils for hydrophobic guests [47].

Synchrotron small-angle X-ray-scattering (SAXS) experiment for the aqueous solution of **Ru-f-6Np** (1.0 mM) and CB[8] (1:3) revealed a broad, but discernible peak (Figure 3a), which matched well with the calculated $\{100\}$ d-spacing (3.0 nm) of the modelled network obtained according to the reported method [31], and supported that the above-mentioned nanoscale supramolecular entity existed as a regular or periodic porous framework (**MSP-f-6Np**, Figure 3) or supramolecular organic framework. The broadness of the peak may be attributed to the dynamic nature of the self-assembled systems in solution [31], although defects could not be excluded. The synchrotron SAXS profile for the solid microcrystals, obtained by slow evaporation of the above solution and evidenced by TEM images (Figure S6, ESI), gave rise to two stronger and sharper peaks (Figure 4b), which matched with the calculated $\{110\}$ and $\{111\}$ spacings (2.1 and 1.7 nm) of **MSP-f-6Np**. The peaks could also be observed from the 2D SAXS profile (Figure 4b, inset). These results indicate that the periodicity of **MSP-f-6Np** was also

maintained and the $(\text{Np})_2\text{C}[\text{CB}[8]]$ binding motif did not change in the solid state. Elemental mapping analysis confirmed the composition of the C, N, Cl, O and Ru elements in the microcrystals (Figure S7, ESI).

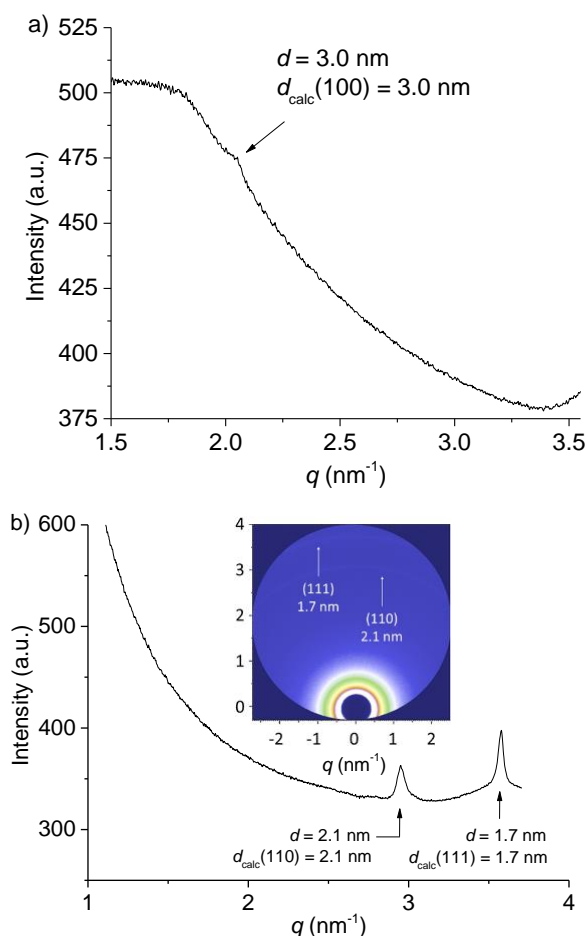


Figure 4 a) Solution-phase synchrotron SAXS profile of **MSP-f-6Np** formed by **Ru-f-6Np** (1.0 mM) and **CB[8]** (1:3) in water and b) synchrotron SAXS profile of the **MSP-f-6Np** microcrystals formed by evaporation of the above solution (Inset: 2D profile). Both of which confirmed the periodicity of **MSP-f-6Np**.

Molecular modelling revealed that **MSP-f-6Np** possesses about 75% of void volume and the pore aperture of the square defined by four adjacent **CB[8]** molecules was about 1.4 nm (Figure 3). To test the stability of this new highly ordered supramolecular polymer formed from a structurally flexible monomer as well as to explore the function of the $[\text{Ru}(\text{bipy})_3]^{2+}$ complexes incorporated in the monomer, we first studied the influence of organic dyes, including methylene blue (**MB**), congo red (**CR**) and crystal violet (**CV**) (Figure 1), on the fluorescence of the $[\text{Ru}(\text{bipy})_3]^{2+}$ complexes. Adding these dyes to the aqueous solution of **MSP-f-6Np** caused complete or significant quenching of the fluorescence of the framework (Figures S8-S10, ESI), whereas for the solution of **Ru-f-6Np**, quenching also took

place, but all with a pronouncedly lower efficiency. It has been reported that **CB[8]** is able to encapsulate **MB** or other organic dyes in water [48-50]. DLS studies revealed that adding linear **MB** and **CR** (1.0 mM) to the solution of **MSP-f-6Np** ($[\text{Ru-f-6Np}] = 0.3 \text{ mM}$) in water did not cause a significant change of the D_{H} value after the solutions were stayed for 1 hour, which indicated that the dyes did not decompose the polymer frameworks through entering the cavity of the **CB[8]**. This result is not unexpected considering that the binding between **CB[8]** and the Np units of **Ru-f-6Np** displayed important multivalence. The fact that both cationic and anionic dyes more efficiently quenched the fluorescence of the $[\text{Ru}(\text{bipy})_3]^{2+}$ complexes of **MSP-f-6Np** than the pure complex **Ru-f-6Np** supported that the dyes were adsorbed into the pores of the **MSP-f-6Np**. **MSP-f-6Np** can be considered as a new porous ordered cationic supramolecular polyelectrolyte. The adsorption for cationic **MB** and **CV** should be driven mainly by hydrophobicity, even though the process for **CR** might be also promoted by ionic electrostatic interaction.

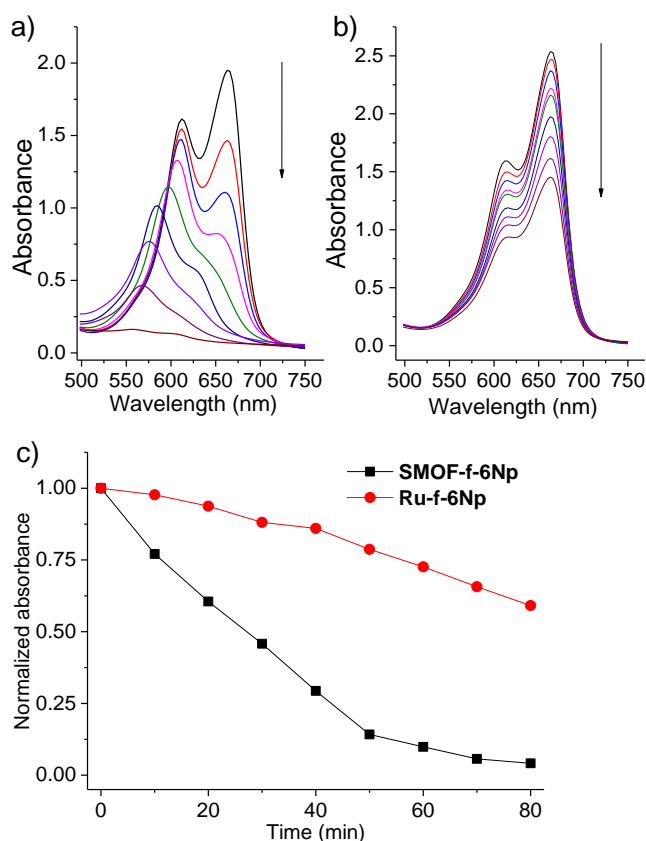


Figure 5 Visible light-induced change of the UV-vis spectra of methylene blue (**MB**) (0.05 mM) in the aqueous solution of a) **MSP-f-6Np** and b) **Ru-f-6Np** at 25 °C ($[\text{Ru}^{2+}] = 0.01 \text{ mM}$), and c) normalized absorbance vs irradiation time.

Irradiating the aqueous solution of **MB** in the presence of **MSP-f-6Np** caused complete degradation of the dye in 80 minutes (Figures 5a and 5c). In contrast, after the identical

irradiation time, **Ru-f-6Np** of the same concentration could lead to only 41% of the dye to degrade (Figures 5b and 5c). Similar enhanced catalysis of **MSP-f-6Np** for the degradation of **CR** and **CV** was also observed (Figures S11 and S12, ESI). These results indicated that the Ru₂⁺ complexes as the nodes of the cubic framework catalyzed the degradation of the dyes in a cooperative manner. The heterogeneous catalysis of **MSP-f-6Np** for the degradation of **MB** in acetonitrile revealed that, after 5 hours of visible light irradiation, **MB** was degraded completely (Figure S13, ESI). However, with **Ru-f-6Np** of the same molar amount as catalyst, only 58% of **MB** was degraded. The activity enhancement of **MSP-f-6Np** may be attributed to the fact that the framework prevented the aggregation of the Ru₂⁺ complexes and as a result, the catalysis could take place as in a homogeneous system despite a slightly lower efficiency.

3 Conclusions

In conclusion, we have demonstrated that a highly ordered porous metallo-supramolecular polymer can be assembled from a flexible six-armed ruthenium complex building block through the encapsulation of CB[8] for the dimers of the appended naphthalene units. The new porous regular supramolecular polymer is highly stable in water to allow for enhanced photodegradation of organic dyes at very dilute concentration under both homo- and heterogeneous conditions. The principle established herein should be applicable to other kinds of multi-armed flexible monomers to construct new well-defined porous MSPs or supramolecular organic frameworks (SOFs), and the resulting regular porous materials may be further exploited as new biocompatible porous materials for adsorbing and transporting biologically active species.

Acknowledgments This work was supported by NSFC (21432004, 21529201 and 21890732). YL thanks the support from The Molecular Foundry, a national user facility supported by the Office of Science, Office of Basic Energy Sciences, of the U.S. Department of Energy under Contract No. DE-AC02-05CH11231. We are also grateful for Shanghai Synchrotron Radiation Facility for providing the beam time (beamlines BL16B1 and BL14B1). Solution SAXS data was collected at the Advanced Light Source (ALS), SIBYLS beamline on behalf of US DOE-BER, through the Integrated Diffraction Analysis Technologies (IDAT) program. Additional support comes from the NIGMS project ALS-ENABLE (P30 GM124169) and a High-End Instrumentation Grant S10OD018483.

Conflict of interest The authors declare that they have no conflict of interest.

Supporting information The supporting information is available online at <http://chem.scichina.com> and <http://link.springer.com/journal/11426>.

- 1 Fouquey C, Lehn JM, Levelut AM. *Adv Mater*, 1990, 2: 254–257
- 2 Brunsveld L, Folmer BJB, Meijer EW, Sijbesma RP. *Chem Rev*, 2001, 101: 4071–4097
- 3 Fox JD, Rowan SJ. *Macromolecules*, 2009, 42: 6823–6835
- 4 Guo DS, Liu Y. *Chem Soc Rev*, 2012, 41: 5907–5921
- 5 Appel EA, del Barrio J, Loh XJ, Scherman OA. *Chem Soc Rev*, 2012, 41: 6195–6214

- 6 Wang Z, Liao S, Wang Y. *Chin J Polym Sci*, 2018, 36: 288–296
- 7 Wei P, Yan X, Huang F. *Chem Soc Rev*, 2015, 44: 815–832
- 8 Hendrikse SIS, Wijnands SPW, Lafleur RPM, Pouderoijen MJ, Janssen HM, Dankers PYZ, Meijer WW. *Chem Commun*, 2017, 53: 2279–2282
- 9 Yin ZJ, Wu ZQ, Lin F, Qi QY, Xu XN, Zhao X. *Chin Chem Lett*, 2017, 28: 1167–1171
- 10 Lu Z, Tang L. *Chem Res Chin Univ*, 2018, 34: 849–856
- 11 Adhikari B, Lin X, Yamauchi M, Ouchi H, Aratsu K, Yagai S. *Chem Commun*, 2017, 53: 9663–9683
- 12 Tian W, Li X, Wang J. *Chem Commun*, 2017, 53: 2531–2542
- 13 Chen Y, Huang F, Li ZT, Liu Y. *Sci China Chem*, 2018, 61: 979–992
- 14 Feng W, Jin M, Yang K, Pei Y, Pei Z. *Chem Commun*, 2018, 54: 13626–13640
- 15 Chen Y, Sun S, Lu D, Shi Y, Yao Y. *Chin Chem Lett*, 2019, 30: 37–43
- 16 Mulder A, Huskens J, Reinhoudt DN. *Org Biomol Chem*, 2004, 2: 3409–3424
- 17 Xu JF, Chen L, Zhang X. *Chem Eur J*, 2015, 21: 11938–11946
- 18 Tian J, Chen L, Zhang DW, Liu Y, Li ZT. *Chem Commun*, 2016, 52: 6351–6362
- 19 Yang B, Zhang XD, Li J, Tian J, Wu YP, Yu FX, Wang R, Wang H, Zhang DW, Liu Y, Zhou L, Li ZT. *CCS Chem*, 2019, 1: 156–165
- 20 Tian J, Wang H, Zhang DW, Liu Y, Li ZT. *Natl Sci Rev*, 2017, 4: 426–436
- 21 Wu YP, Yang B, Tian J, Yu SB, Wang H, Zhang DW, Liu Y, Li ZT. *Chem Commun*, 2017, 53: 13367–13370
- 22 Waller PJ, Gandara F, Yaghi OM. *Acc Chem Res*, 2015, 48: 3053–3063
- 23 Cao L, Wang T, Wang C. *Chin J Chem*, 2018, 36: 754–764
- 24 Han Z, Shi W, Cheng P. *Chin Chem Lett*, 2018, 29: 819–822
- 25 Liu Y, Liu B, Zhou Q, Zhang T, Wu W. *Chem Res Chin Univ*, 2017, 33: 971–978
- 26 Yang T, Cui Y, Chen H, Li W. *Huaxue Xuebao*, 2017, 75: 339–350
- 27 Ding SY, Wang W. *Chem Soc Rev*, 2013, 42: 548–568
- 28 Yuan F, Tan J, Guo J. *Sci China Chem*, 2018, 61: 143–152
- 29 Wu MX, Yang YW. *Chin Chem Lett*, 2017, 28: 1135–1143
- 30 Liu G, Sheng J, Zhao Y. *Sci China Chem*, 2017, 60: 1015–1022
- 31 Tian J, Xu ZY, Zhang DW, Wang H, Xie SH, Xu DW, Ren YH, Wang H, Liu Y, Li ZT. *Nat Commun*, 2016, 7: 11580
- 32 Li XF, Yu SB, Yang B, Tian J, Wang H, Zhang DW, Liu Y, Li ZT. *Sci China Chem*, 2018, 61: 830–835
- 33 Ko YH, Hwang I, Lee DW, Kim K. *Israel J Chem*, 2011, 51: 506–514
- 34 Liu Y, Yang H, Wang Z, Zhang X. *Chem Asian J*, 2013, 8: 1626–1632
- 35 Yang X, Liu F, Zhao Z, Liang F, Zhang H, Liu S. *Chin Chem Lett*, 2018, 29: 1560–1566
- 36 Zou H, Liu J, Li Y, Li X, Wang X. *Small*, 2018, 14: 1802234
- 37 Winter A, Schubert US. *Chem Soc Rev*, 2016, 45: 5311–5357
- 38 Hou Z, Dehaen W, Lyskawa J, Woisel P, Hoogenboom R. *Chem Commun*, 2017, 53: 8423–8426.
- 39 Yin G, Chen L, Wang C, Yang H. *Chin J Chem*, 2018, 36: 134–138
- 40 Bentz KC, Cohen SM. *Angew Chem Int Ed*, 2018, 57: 14992–15001
- 41 Ding Z, Li H, Gao W, Zhang Y, Liu C, Zhu Y. *Chin J Chem*, 2017, 35: 447–456
- 42 Wu D, Xu F, Sun B, Fu R, He H, Matyjaszewski M. *Chem Rev*, 2012, 112: 3959–4015
- 43 Liu H, Kan XN, Wu CY, Pan QY, Li ZB, Zhao YJ. *Chin J Polym. Sci*, 2018, 36: 425–444
- 44 Beuerle F, Gole B. *Angew Chem Int Ed*, 2018, 57: 4850–4878
- 45 Huang Z, Yang L, Liu Y, Wang Z, Scherman OR, Zhang X. *Angew Chem Int Ed*, 2014, 53: 5351–5355
- 46 Lee JW, Samal S, Selvapalam N, Kim HJ, Kim K. *Acc Chem Res*, 2003, 36: 621–630
- 47 Biedermann F, Nau WM, Schneider HJ. *Angew Chem Int Ed*, 2014, 53: 11158–11171
- 48 Montes-Navajas P, Corma A, Garcia H. *ChemPhysChem*, 2008, 9: 713–720
- 49 Sun S, Li F, Liu F, Wang J, Peng X. *Sci Rep*, 2014, 4: 3570
- 50 Xu Z, Lian X, Li M, Zhang X, Wang Y, Tao Z, Zhang Q. *Chem Res Chin Univ*, 2017, 33: 736–741